

Rainbows in Energy- and Angle-Resolved Ion Scattering from Surfaces

A. D. Tenner, K. T. Gillen,^(a) T. C. M. Horn, J. Los, and A. W. Kleyn

FOM Institute for Atomic Molecular Physics, Kruislaan 407, 1098 SJ Amsterdam, The Netherlands

(Received 24 February 1984)

The angular and energy distributions of K^+ ions scattered at normal incidence with an initial energy of 35 eV on a W(110) surface were measured for various crystal orientations. The complex distributions show rainbows which are due both to extrema in the deflection functions for the two scattering angles as well as to an extremum in the final energy as a function of the impact parameter. With use of computer simulations with a nonadditive model potential all observed structures can be explained.

PACS numbers: 79.20.Nc, 34.50.-s, 68.20.+t, 82.65.Nz

The occurrence of rainbows is a well-known phenomenon in scattering processes, first of all from rainbows in the sky. But also in atom scattering in the gas phase,¹ in atom scattering from strings of atoms in surfaces,² in rotationally inelastic surface scattering,³ and in scattering of heavy nuclei in nuclear physics⁴ rainbows are known. The origin of the rainbow in scattering processes is an extremum in the classical deflection function which gives rise to an infinite cross section. In the cases mentioned above this singularity occurs in a single-differential cross section, but also in double-differential cross sections this kind of singularity occurs, e.g., rotational rainbows in atom-molecule collisions¹ and surface rainbows in scattering from a two-dimensional lattice.^{2,5,6} In all of these cases the rainbow structure gives detailed information on the dynamics of the scattering process and the underlying interaction potential. In this paper we will report the first observations of rainbow structure in triple-differential cross sections. This is realized in energy- and angle-resolved surface scattering experiments. The system studied is K^+ on W(110) at 35 eV.

Alkali ion scattering at 35 eV lies between scattering at thermal energies exhibiting complicated energy transfer with trapping and/or desorption⁷ and structure scattering at high energies (> 250 eV).⁸ The present energy is high enough to prevent trapping⁹ and low enough to prevent penetration¹⁰ of the surface. To obtain scattering profiles that are easy to interpret and that give information about the entire potential, we have considered the following points: (1) Experiments have been carried out using alkali ions as projectiles, because beams of these ions are easily prepared and neutralization does not occur.¹¹ In addition these ions have a closed-shell noble gas configuration. (2) The incoming beam is always normal to the surface and the scattered signal can be detected along the two angles θ and ϕ , where θ is the polar scattering angle

with respect to the surface normal and ϕ is the azimuthal angle; $\phi = 0$ corresponds to the [110] direction in the surface (see inset of Fig. 1). Thus there are no blocking effects of the incoming beam and there is no incident velocity parallel to the surface plane. This facilitates the analysis because the surface is fully exposed to the beam. (3) K^+ ions have been chosen as projectiles for a W(110) surface because the mass ratio is 0.21, which means a reasonable momentum transfer. So different scattering paths not only lead to different θ and ϕ , but also to differences in energy after the collision (E'). From the triple-differential cross section presented here very detailed information about the collision dynamics and the interaction potential can be extracted. The data and analysis will be described in more detail elsewhere.¹² We note that in contrast to measuring energy-loss spectra at some selected geometries,^{7,8} we map the entire differential cross section.

The experimental apparatus consists of a ultra-high-vacuum (UHV) chamber with a base pressure of 10^{-8} Pa. In the UHV chamber a K^+ ion source with a lens system is mounted. The target is a W(110) surface which is cleaned in the usual way (annealing in oxygen and flashing to 2500 K). The crystal is mounted on a two-axes goniometer. The detector consists of a 90° electrostatic analyzer with $\Delta E/E = 0.08$, rather large to ensure a reasonable transmission for the low-energy ions. It is rotatable around two axes. This allows scattering angles from 17° to 180° with respect to the primary beam in the detection plane and 90° out of plane. The angular resolution of the system is in the order of 0.5° .

Figures 1–3 give the experimental results. The scattered intensity, not corrected for the transmission of the energy analyzer, is plotted as a function of θ and E' for three azimuthal angles. The figures show a complicated peak structure in the triple-differential cross section that can be attributed to different types of scattering paths. In order to iden-

tify the structures, classical trajectory calculations have been performed.

In the simulations, trajectories of the scattered particles are calculated by integration of Newton's equations. The projectile interacts with all atoms of the target simultaneously, for at these low energies the interaction cannot be described by consecutive collisions. The number of target atoms that take part in the interaction is at least five, the four atoms of the surface unit cell and one atom of the second layer. For the present discussion we take the target atoms to be initially at rest. The potential used is the sum of pairwise Born-Mayer repulsive terms and an attractive image-potential term. This potential form gives a corrugated potential hypersurface. Calculations with this potential, however, cannot reproduce the position of peak *a* of Fig. 1. This can be overcome by allowing the Born-Mayer potential for the second-layer atoms to be quite different from those of the surface atoms. This means that in the energy range discussed here, addition of identical pair potentials does not give the right

overall shape for the potential. Because the potential is related to the electron density,¹³ an increase of the potential for the second-layer atoms means an increase in electron density in the center of the unit cell. This effect is also indicated by Hulpke and Mann,⁶ and by electron-density calculations by Wimmer *et al.*¹⁴ At this moment, our calculations show qualitatively the same structure as the experimental results, all features are present in the right positions, but to get a better fit of the experimental results, we are still improving the calculations as will be described in detail elsewhere.¹²

To interpret the peaks one can construct deflection functions in three dimensions from the calculations. From these deflection functions the origin of the structures can be obtained with use of an appropriate definition of the triple-differential cross section $\sigma(\theta, \phi, E')$. Following Beck, Ross, and Schepper¹⁵ we define

$$\sigma(\theta, \phi, E') \sin\theta d\theta d\phi dE' = dx dy dE,$$

where E is the primary beam energy and x, y are the

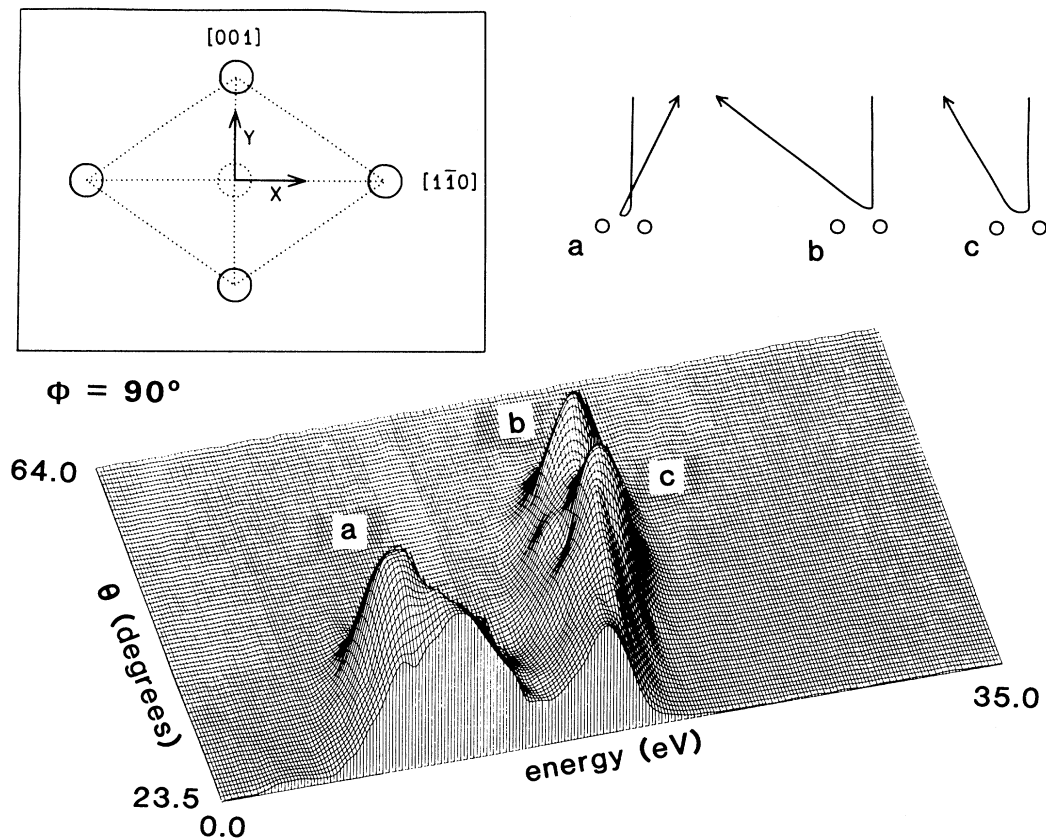


FIG. 1. Measured distribution of the scattered intensity of the K^+ ions for an incident energy of 35 eV as a function of the scattering angle θ and the energy after the collision E' , for a fixed azimuthal angle $\phi = 90^\circ$. The inset shows a schematic picture of the W(110) surface and *a*, *b*, and *c* show the kinds of collisions that cause the different peaks in the distribution.

coordinates of the two-dimensional impact parameter: The x and y axes are defined in the inset of Fig. 1. Rainbowlike structures arise when $\sin\theta \neq 0$ and the Jacobian determinant is zero

$$\det J = \partial(\theta, \phi, E')/\partial(x, y, E) = 0.$$

If one assumes that the scattering angles are independent of energy this expression reduces to the well-known condition for surface rainbows $\partial(\theta, \phi)/\partial(x, y) = 0$. Several conditions exist to obtain $\det J = 0$, thus giving rise to rainbows, i.e., singularities in three-dimensional detection space.

Turning to the experimental results: The structure observed is complicated for $\phi = 90^\circ$ (Fig. 1), i.e., for those ions that are scattered parallel to the [001] direction or y axis. The computer simulations indicate that most of the intensity observed for $\phi = 90^\circ$ is due to impact parameters along the y axis. So called zig-zag collisions⁸ also contribute to the scattering, but they do not give rise to additional features and will be ignored in the present discussion. From the symmetry of the unit cell it immediately follows that in this case $\partial\theta/\partial x = \partial E'/\partial x = \partial\phi/\partial y = 0$. $\det J = 0$ can be obtained when $\partial\phi/\partial x = 0$, which is not the case, or when $\partial\theta/\partial y = \partial E'/\partial y = 0$. The latter partial derivatives have roots along the y axis but not simultaneously, so $\det J \neq 0$. Therefore a real rainbow cannot be obtained but local extrema can.

The condition $\partial\theta/\partial y = 0$, leading to a maximum in scattering angle, occurs for impact parameters for which after a single collision with one target atom the projectile starts to hit the second atom (type b ,

Fig. 1). Near the center of the unit cell more violent encounters, leading to "backward" scattering, are possible (type a) and this collision also makes $\partial\theta/\partial y = 0$. Without energy analysis of the product the two roots of $\partial\theta/\partial y$ mentioned lead to two types of surface rainbows as discussed in the work of Hulpke and co-workers.^{5,6}

A maximum in E' , $\partial E'/\partial y = 0$, occurs when the double collision is as symmetric as possible with a minimum energy loss. This gives rise to another peak in the spectrum (peak c), which almost completely disappears when only the angular distributions of the scattered ions are measured. It is important to note that this feature has not been identified before and that it is not the same as the well-known "single and double" collision peaks which are observed in energy-loss spectra.⁸ These peaks are not resolved in the present measurements due to the moderate resolution of the energy analyzer, but are found in the computer simulations.

When we go away from the y axis the structure disappears due to a lack of symmetry of the potential hypersurface. However, for scattering at $\phi = 70^\circ$ structure reappears. For this direction without symmetry in the crystal it happens that $\partial\theta/\partial x = \partial\theta/\partial y = \partial\phi/\partial x = \partial\phi/\partial y = 0$, so $\det J = 0$, giving rise to a real rainbow (Fig. 2) which is clearly visible. Evidently there is a focusing effect leading to a "channel" inside the unit cell between two close-packed target atoms.

If the azimuthal angle is decreased further, the structure disappears again. When the atoms are scattered parallel to the x axis ($\phi = 0$), (Fig. 3), we

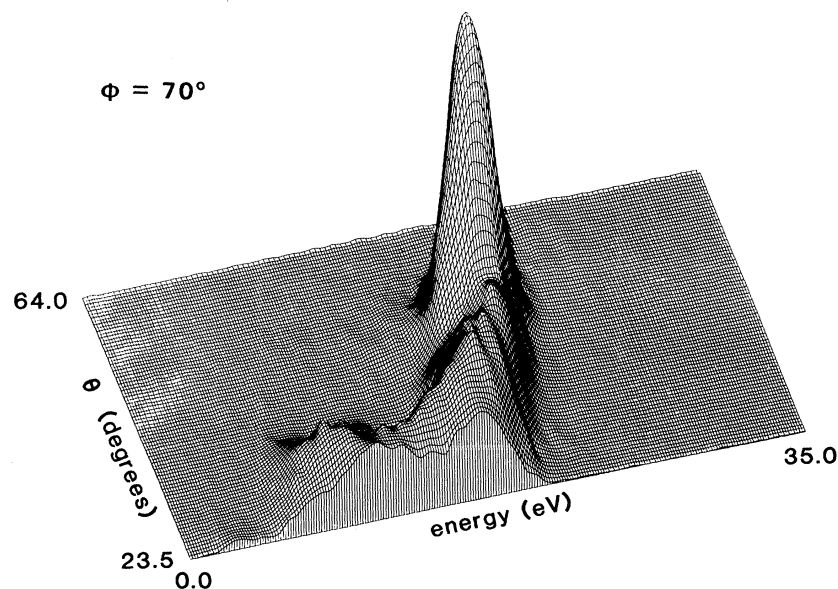


FIG. 2. Measured distribution as in Fig. 1, for $\phi = 70^\circ$.

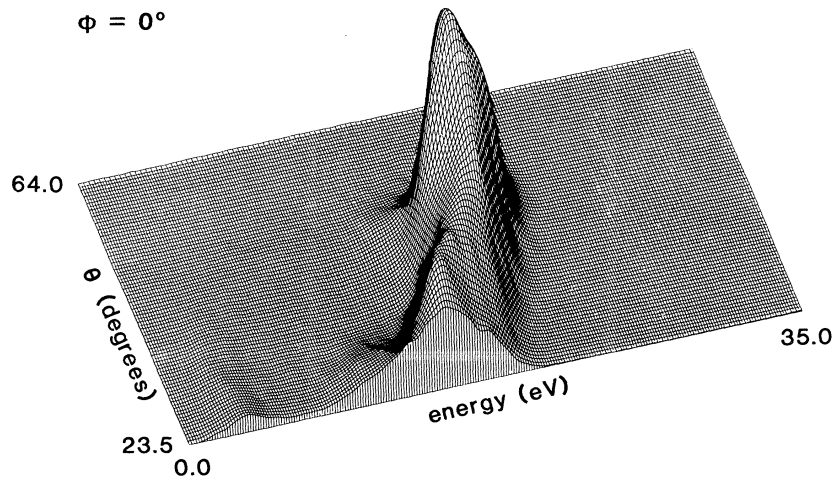


FIG. 3. Measured distribution as in Fig. 1, for $\phi = 0^\circ$.

have a similar symmetry as for $\phi = 90^\circ$, but in this case no type-*a* collisions are possible due to a larger atomic distance in the lattice string. Furthermore the maxima from type-*b* and type-*c* collisions come so close together that they merge, i.e., $\partial\theta/\partial x = \partial E'/\partial x = 0$, again a real rainbow in the triple-differential cross section.

Summarizing, we have demonstrated for the first time that rainbows can indeed be observed in measurements of triple-differential cross sections for K^+ ions scattered from W(110). In addition to the peaks due to angular rainbows, peaks have been found which are due to extrema in the final energy E' as a function of the impact parameter. Analysis of these features with classical trajectory calculations gives an insight into the interaction potential between the ion and a metal surface; the method is not limited to W(110). The occurrence and location of rainbows is very sensitive to the shape of the potential, therefore rainbow analysis can be used as a tool in determining the potential. This interaction potential governs the dynamics of several surface phenomena such as chemisorption and surface ionization. It cannot be described by a sum over identical pairwise interaction potentials.

This work is sponsored by the Fundamenteel Onderzoek der Materie with financial support by the Nederlandse Organisatie voor Zuiver-Wetenschappelijk Onderzoek.

^(a)Present address: SRI International, 333 Ravenswood Avenue, Menlo Park, California 94025.

¹R. Schinke and J. M. Bowman, in *Molecular Collision Dynamics*, edited by J. M. Bowman (Springer-Verlag,

Berlin, 1983), p. 61-115.

²F. O. Goodman and H. Y. Wachman, *Dynamics of Gas-Surface Scattering* (Academic, New York, 1976), Chap. 7.

³See, e.g., J. A. Barker, A. W. Kleyn, and D. J. Auerbach, *Chem. Phys. Lett.* **97**, 9 (1983).

⁴M. Buenard, P. Martin, R. Bertholet, C. Guet, M. Maurel, J. Mougey, H. Nifenecker, J. Pinston, P. Perrin, F. Schussler, J. Julien, J. P. Bondorf, L. Carlen, H. Å. Gustafsson, B. Jakobsson, T. Johansson, P. Kristiansson, O. B. Nielsen, A. Oskarsson, I. Otterlund, H. Ryde, B. Schröder, and G. Tibell, *Phys. Rev. C* **26**, 1299 (1982).

⁵U. Gerlach-Meyer and E. Hulpke, in *Topics in Surface Chemistry*, edited by E. Kay and P. S. Bagus (Plenum, New York, 1978), p. 195-223; U. Gerlach-Meyer, E. Hulpke, and H.-D. Meyer, *Chem. Phys.* **36**, 327 (1979).

⁶E. Hulpke and K. Mann, *Surf. Sci.* **133**, 171 (1983).

⁷M. J. Cardillo, *Annu. Rev. Phys. Chem.* **32**, 331 (1981).

⁸T. von dem Hagen and E. Bauer, *Phys. Rev. Lett.* **47**, 579 (1981); T. von dem Hagen, M. Hou, and E. Bauer, *Surf. Sci.* **117**, 134 (1982).

⁹A. Hurkmans, E. G. Overbosch, D. R. Olander, and J. Los, *Surf. Sci.* **54**, 154 (1976).

¹⁰E. G. Overbosch, A. D. Tenner, and J. Los, *Radiat. Eff.* **53**, 73 (1980).

¹¹A. Hurkmans, E. G. Overbosch, K. Kodera, and J. Los, *Nucl. Instrum. Methods* **132**, 453 (1976).

¹²A. D. Tenner, K. T. Gillen, T. C. M. Horn, J. Los, and A. W. Kleyn, to be published.

¹³N. Esbjerg and J. K. Norskov, *Phys. Rev. Lett.* **45**, 807 (1980).

¹⁴E. Wimmer, A. J. Freeman, M. Weinert, H. Krakauer, J. R. Hiskes, and A. M. Karo, *Phys. Rev. Lett.* **48**, 1128 (1982).

¹⁵D. Beck, U. Ross, and W. Schepper, *Z. Phys. A* **293**, 107 (1979).